Journal of Information & Optimization Sciences
ISSN 0252-2667 (Print), ISSN 2169-0103 (Online)
Vol. 45 (2024), No. 1, pp. 73–94
DOI : 10.47974/JIOS-1271

Modeling, analyzing and simulating the dynamics of Tuberculosis-Covid-19 co-infection

Haileyesus Tessema Alemneh *
Department of Mathematics
College of Natural and Computational Sciences
University of Gondar
Gondar
Ethiopia

Zinabu Teka Melese
Department of Statistics
College of Natural and Computational Sciences
University of Gondar
Gondar
Ethiopia

Abstract

Covid-19 and tuberculosis (TB) are two significant infectious illnesses that may pose significant threats to the public health and their co-infection aggravates the issue. Through the use of a set of nonlinear ordinary differential equations and contaminated surfaces from SARS-CoV-2 in the environment, we developed and investigated a mathematical model in this study for the dynamics of the co-infection of Covid-19 and TB transmission. The free equilibrium point of the disease was determined and its stability was investigated. The next generation matrix approach is used to determine the model's basic reproduction number. The disease-free equilibrium point is not globally asymptotically stable, but it is locally asymptotically stable if $\mathcal{R}_0 < 1$. We found key model parameters for disease dynamics spread using normalized forward sensitivity analysis. From the numerical simulation results, we conclude that government stakeholders should work in reducing the transmission mechanisms of both diseases. In addition, they should look on mechanisms for removing SARS-CoV-2 contaminated surfaces from the community.

Subject Classification: *34D35, 37C75, 65L06.*

Keywords: *Covid-19, TB, Co-infection, Mathematical model, Stability analysis, Numerical simulation.*

* *E-mail:* **haila.tessema@gmail.com (Corresponding Author)**

1. Introduction

The coronavirus infection (Covid-19) has been deemed a global public health emergency since it was first found in Wuhan, China in 2019 [1]. Covid-19 is a single-stranded ribonucleic acid (RNA) virus that is caused by the severe acute respiratory syndrome corona virus 2 (SARS-CoV-2) [1, 2]. The SARS-CoV 2 can be transmitted directly by droplets that escape the lungs through coughing or sneezing from an infected humans [3]. Additionally, when a person touches a surface that has been contaminated by the virus, they could get sick [4]. The WHO situation report states that since the Covid-19 outbreak, more than 245,310,625 persons have been infected globally, 4,979,526 have died and about 222,399,916 have recovered [2].

According to WHO health statistics, tuberculosis is one of the top 10 major causes of death worldwide, annually infecting nearly one-third of the global population[5]. From a report by the WHO [5], millions of people worldwide die from tuberculosis each year and millions more develop the disease [5, 6]. Globally, it is predicted that 10 million individuals would contract tuberculosis (TB) in 2020 of which 3.6 million women, 1.1 million children and 5.6 million men[5]. Mycobacterium tuberculosis (MTB) is responsible for tuberculosis (TB) infection which primarily affects the lungs (pulmonary TB) [6]. Tuberculous meningitis (TBM) is an extra-pulmonary form of tuberculosis (TB) characterized by sub-acute or chronic inflammation of the meninges as a result of invasion of the sub-arachnoid space by the *bacilli M.* Tuberculosis [7]. It is the most severe form of TB and has the highest mortality and morbidity rate compared to other forms of TB [8]. The highest risk populations are children under 5 years of age, the HIV co-infected and immuno compromised [8, 9].

Coinfection with severe acute respiratory syndrome-associated coronavirus 2 (SARS-CoV-2) and Mycobacterium tuberculosis has been reported in various parts of the world [10]. The TB patients with Covid-19 are at higher risk of developing severe disease and may become critically ill requiring mechanical ventilation [11]. The rate of severe Covid-19 is higher among TB patients, the program needs to focus of primary prevention measure and preferable airborne control measures needs to be maintained in all TB care centers to reduce the risk of transmission of SARS-CoV2 infection [12]. The TB treatment centers and hospitals need to be prepared for early identification and management of Covid-19 in TB patients [13]. Additionally, the HIV/TB co-infected group has the highest risk in the Covid-19 mortality rate and poor recovery rate [14]. Although it is rare, coinfection with severe acute respiratory syndrome-

associated coronavirus 2 (SARS-CoV-2) and Mycobacterium tuberculosis (MBT) has been reported in various parts of the world[10–12]. The first-ever global cohort of 49 cases of TB-Covid-19 co-infection from 8 countries were reported [11]. Mycobacterium tuberculosis (MTB) and Covid-19 coinfection have been documented. In addition it has been researched that SARS-CoV-2 is seen on tuberculous meningitis (TBM) patients, which is most fatal form of TB that occurs in 1-5% of those with TB [15].

To better understand the dynamics of communicable disease transmission and to give public health policy makers guidance on how to choose effective intervention programs to combat infections, mathematical models for infectious diseases can be employed. Various dynamical models have been established and evaluated to distinguish the most crucial variables that aid in predicting the trends of infectious diseases and their preventative measures of TB and COVID 19 disease transmission. For illustration, to understand the Covid-19 epidemic, mathematical models with different aims were created and examined by [19, 21–28]. Similar to this, numerous TB dynamical models are investigated and proposed by [16–20]. Also, some co-infection models for TB and HBV [29], HIV-TB can be found in [30]. The coinfection of Cholera-Covid-19 in [31], Dengue-Covid-19 in [32], Malaria-Covid-19 in [33] and coinfection Covid-19 with other disease [34, 35]. Recently a fractional-order model for Covid-19 and tuberculosis co-infection using Atangana-Baleanu derivative has been studied by [36]. They assumed the susceptible individuals were infected following successful encounters with Covid-19 infected exposed and co-infected persons. However, in our proposed model, we presupposed that susceptible people become infected after having direct encounters with Covid-19 infected or co-infected individuals as well as getting contact with contaminated surfaces or objects in the environment.

The following is how the paper is arranged: The mathematical model of the TB-Covid-19 coinfection is described in Section 2 along with a list of definitions and some fundamental underlying assumptions. The mathematical model of TB-Covid-19 co-infection is presented in Section 3. Section 4 shows the investigation of the mathematical model and explores its fundamental features. Numerical simulations were given in Section 5 to strengthen the information from analytical results. The discussion and conclusions are covered in the final Section 6.

2. Baseline Model Formulation

To achieve the main aim of this study, we develop, analyze and simulate an epidemic model that describes the transmission dynamics

of TB- Covid-19 coinfection. According to human disease status, the total human population into seven different epidemiological classes depending on individuals health status: susceptible humans $\mathcal{S}$, infectious individuals with TB $\mathcal{I}_m$, individuals who have recovered from TB $\mathcal{R}_m$, infectious individuals with Covid-19 $\mathcal{I}_c$, individuals who have recovered from Covid-19 $\mathcal{R}_c$, infectious individuals with co-infected with TB and Covid-19 $\mathcal{I}_{cm}$. Individuals who have recovered from co-infected with TB and Covid-19 $\mathcal{R}_{cm}$. The contaminated surfaces by the SARS-CoV-2 virus in the environmental is given by $\mathcal{P}$ is considered in the disease transmission dynamics. The model has the following assumptions:

(i) People who are susceptible can get Covid-19 if they come into contact with infected or co-infected people and they can contract TB if they come into contact with infected or co-infected people.

(ii) Persons with Covid-19 infections are vulnerable to TB infections and vice versa.

(iii) Co-infected patients can spread either TB or Covid-19 but not both illnesses simultaneously.

(iv) People who are co-infected can recover from Covid-19, TB and mixed infections all at once.

(v) It is presumed that both co-infected persons and those who are infected alone have the same rate of transmissibility.

Ω is the rate at which individuals are introduced into the population through birth or immigration.

Following successful interactions with Covid-19-infected persons who are either single or co-infected, susceptible humans, $\mathcal{S}$, acquire Covid-19 at the rate of

$$\lambda_1 = \frac{\beta(\mathcal{I}_c + \mathcal{I}_{cm} + \varepsilon\mathcal{P})}{N}$$

Similarly, the population is reduced due to infection with TB at the rate: Similarly, TB infection reduces the population $\mathcal{S}$ at a rate of

$$\lambda_2 = \frac{\alpha(\mathcal{I}_m + \mathcal{I}_{cm})}{N}$$

Following the assumptions above, we present below deterministic systems of nonlinear ordinary differential equations, to study the transmission dynamics of TB-Covid-19 co-infection.

$$\begin{cases} \frac{d\mathcal{S}}{dt} &= \Omega + \delta_2\mathcal{R}_m + \delta_1\mathcal{R}_c + \delta_3\mathcal{R} - (\lambda_1+\lambda_2)\mathcal{S} - \mu\mathcal{S} \\ \frac{d\mathcal{I}_c}{dt} &= \lambda_1\mathcal{S} - \lambda_2\mathcal{I}_c - (\eta_1+\sigma_1+\mu)\mathcal{I}_c \\ \frac{d\mathcal{I}_m}{dt} &= \lambda_2\mathcal{S} - \lambda_1\mathcal{I}_m - (\eta_2+\sigma_2+\mu)\mathcal{I}_m \\ \frac{d\mathcal{I}_{cm}}{dt} &= \lambda_2\mathcal{I}_c + \lambda_1\mathcal{I}_m - (\varphi+\sigma+\mu)\mathcal{I}_{cm} \\ \frac{d\mathcal{R}_c}{dt} &= \sigma_1\mathcal{I}_c + \varepsilon\varphi\mathcal{I}_{cm} - (\delta_1+\mu)\mathcal{R}_c \\ \frac{d\mathcal{R}_m}{dt} &= \sigma_2\mathcal{I}_m + (1-\varepsilon)\varphi k\mathcal{I}_{cm} - (\delta_2+\mu)\mathcal{R}_m \\ \frac{d\mathcal{R}_{cm}}{dt} &= \varphi(1-\varepsilon)(1-k)\mathcal{I}_{cm} - (\delta_3+\mu)\mathcal{R}_{cm} \\ \frac{d\mathcal{P}}{dt} &= \vartheta(\mathcal{I}_c+\mathcal{I}_{cm}) - \tau\cdot\mathcal{P} \end{cases} \tag{1}$$

with initial conditions

$$\mathcal{I}(0)\geq 0, \mathcal{I}_c(0)\geq 0, \mathcal{I}_m(0)\geq 0, \mathcal{I}_{cm}(t)\geq 0, \mathcal{R}_c(0)\geq 0, \mathcal{R}_m(0)\geq 0, \mathcal{R}_{cm}(0)\geq 0, \mathcal{P}(0)\geq 0.$$

3. Basic properties of the model

The mathematical model (1) describes the rate of change of different compartments of human populations and it will be epidemiologically significant if all of its state variables are non-negative for all time $t>0$. Hence, we establish the following result.

3.1 *Positivity of Solutions*

Theorem 3.1 : *If* $\mathcal{S}_0>0$, $\mathcal{I}_{c0}>0$, $\mathcal{I}_{m0}>0$, $\mathcal{I}_{cm0}>0$, $\mathcal{R}_{c0}>0$, $\mathcal{R}_{m0}>0$, $\mathcal{R}_{cm0}>0$, $\mathcal{P}_0>0$, *then the future time solutions of the TB-Covid-19 coinfection population is positive .*

Proof: We let $\nu = sup\{t>0 : \mathcal{S}_0(t_1)>0,\ \mathcal{I}_{c0}(t_1)>0,\ \mathcal{I}_{m0}(t_1)>0,\ \mathcal{I}_{cm0}(t_1)>0,\ \mathcal{R}_{c0}(t_1)>0,\ \mathcal{R}_{m0}(t_1)>0,\ \mathcal{R}_{cm0}(t_1)>0,\ \mathcal{P}_0(t_1)>0$ for all $t_1\in[0,t]\}$. Since $\mathcal{S}_0\geq 0,\ \mathcal{I}_{c0}\geq 0,\ \mathcal{I}_{m0}\geq 0,\ \mathcal{I}_{cm0}\geq 0,\ \mathcal{R}_{c0}\geq 0,\ \mathcal{R}_{m0}\geq 0,\ \mathcal{R}_{cm0}\geq 0,\ \mathcal{P}_0\geq 0$, hence $\nu>0$. If $\nu<\infty$, then $\mathcal{S}_0(t),\ \mathcal{I}_{c0}(t),\ \mathcal{I}_{m0}(t),\ \mathcal{I}_{cm0}(t),\ \mathcal{R}_{c0}(t),\ \mathcal{R}_{m0}(t),\ \mathcal{R}_{cm0}(t),\ \mathcal{P}_0(t)$ are zero at t_1. To show solution of the model is positive, first we take $\frac{d\mathcal{S}}{dt}$ from equation (1).

$$\frac{d\mathcal{S}}{dt} = \Omega + \delta_2\mathcal{R}_m + \delta_1\mathcal{R}_c + \delta_3\mathcal{R} - (\lambda_1+\lambda_2-\mu)\mathcal{S} \tag{2}$$

Using the variation of constants formula, the solution of equation (2) at v is given by:

$$\mathcal{S}(v) = \mathcal{S}(0)\exp\left[-\int_0^v((\lambda_1+\lambda_2-\mu)\mathcal{S}(d\mathcal{S})\right] + \int_0^v(\Omega+\delta_2\mathcal{R}_m+\delta_1\mathcal{R}_c+\delta_3\mathcal{R})\exp\left[-\int_{(\mathcal{S}}^v(\lambda_1+\lambda_2-\mu)(t_1)dt_1\right]$$

Moreover, since all the variables are positive in $[0, v]$, then $\mathcal{S}(v) > 0$.

It can be shown in a similar way that $\mathcal{I}_c(v) > 0$, $\mathcal{I}_m(v) > 0$, $\mathcal{I}_{cm}(v) > 0$, $\mathcal{R}_c(v) > 0$, $\mathcal{I}_m(v) > 0$, $\mathcal{R}_{cm}(v) > 0$, $\mathcal{P}(v) > 0$, which is a contradiction. Hence $v = \infty$.

3.2 *Invariant region*

The sum of all the human population in (1) is given by:

$$\frac{d\mathcal{N}}{dt} = \Omega - \mu\mathcal{N} - (\sigma_1\mathcal{I}_c + \sigma_2\mathcal{I}_m + \sigma\mathcal{I}_{cm})$$

If disease specific induced death rates assumed negligible ($\beta = 0 = \alpha$) and no contaminated surface. It is considered that all variables and parameters are nonnegative because model (1) monitors the human population. Hence $0 \le \mathcal{N} \le \frac{\Omega}{\mu}$. Moreover, for the contaminated surfaces in the environmental variable $\mathcal{P}$, we have

$$\frac{d\mathcal{P}}{dt} = \vartheta(\mathcal{I}_c + \mathcal{I}_{cm}) - \tau\cdot\mathcal{P} \le \frac{\vartheta\Omega}{\mu} - \tau\cdot\mathcal{P}$$

By applying the Gronwall inequality, for $0 \le \mathcal{P} \le \frac{\vartheta\Omega}{\tau\mu}$. Therefore, the system (1) will be analyzed in the following invariant region:

$$\Pi = \left\{(\mathcal{S}, \mathcal{I}_c, \mathcal{I}_m, \mathcal{I}_{cm}, \mathcal{R}_c, \mathcal{R}_m, \mathcal{R}_{cm}, \mathcal{P}) \in \mathbb{R}_+^8 : 0, \le \mathcal{N} \le \frac{\Omega}{\mu}, 0 \le \mathcal{P} \le \frac{\vartheta\Omega}{\tau\mu}\right\}$$

Therefore, the model in equation (1) is well-posed mathematically and epidemiologically meaningful.

4. Mathematical analysis of the model

In this section, we analyze model (1) by determining the disease-free equilibrium and basic reproduction the coinfection. We also examines the local and global stability of the disease-free equilibrium. Additionally, we look into the type of bifurcation the model shows and the sensitivity of the parameter values.

4.1 *Disease free equilibrium & Basic reproduction number*

The TB-Covid-19 co-infection has a disease-free equilibrium (DFE) point, which is determined by setting the right-hand sides of the equations in model (1) to zero, which is represented by

$$\mathcal{E}_0 = (\Omega/\mu, 0, 0, 0, 0, 0, 0, 0).$$

In a completely susceptible population, the number of secondary cases that one case would produce is known as a basic reproduction number and denoted by $\mathcal{R}_0$. It is obtained using the next generation approach (see [37, 38]), Using the approach in [37], the associated next generation matrices are given by

$$F_{\mathcal{E}_0} = \begin{pmatrix} \frac{\Omega\beta}{\mu} & 0 & \frac{\Omega\beta}{\mu} & \frac{\beta\varepsilon\Omega}{\mu} \\ 0 & \frac{\Omega\alpha}{\mu} & \frac{\Omega\alpha}{\mu} & 0 \\ 0 & 0 & 0 & 0 \\ 0 & 0 & 0 & 0 \end{pmatrix} \text{ and } \quad V_{\mathcal{E}_0} = \begin{pmatrix} \varsigma_1 & 0 & 0 & 0 \\ 0 & \varsigma_2 & 0 & 0 \\ 0 & 0 & \varsigma_3 & 0 \\ -\vartheta & 0 & -\vartheta & \tau \end{pmatrix}$$

where

$$\varsigma_1 = \vartheta + \eta_1 + \sigma_1 + \mu, \varsigma_2 = \eta_2 + \sigma_2 + \mu, \varsigma_3 = \vartheta + \varphi + \sigma_1 + \sigma_2 + \mu$$

$$FV^{-1} = \begin{pmatrix} \frac{\Omega\beta\tau + \Omega\beta\varepsilon\vartheta}{\mu\tau\varsigma_1} & 0 & \frac{\Omega\beta\tau + \Omega\beta\varepsilon\vartheta}{\mu\varsigma_3} & \frac{\beta\varepsilon\Omega}{\mu\tau} \\ 0 & \frac{\alpha\Omega}{\mu\varsigma_2} & \frac{\alpha\Omega}{\mu\varsigma_3} & 0 \\ 0 & 0 & 0 & 0 \\ 0 & 0 & 0 & 0 \end{pmatrix}$$

Then the spectral radius of the next generation matrix FV^{-1} determines the basic reproduction number corresponding to system (1), which is calculated as

$$\mathcal{R}_{0c} = \frac{\Omega\beta(\varepsilon\vartheta + \tau)}{\mu\tau(\vartheta + \eta_1 + \sigma_1 + \mu)} \qquad \mathcal{R}_{0m} = \frac{\alpha\Omega}{\mu(\eta_2 + \sigma_2 + \mu)}$$

It might additionally be provided as $\mathcal{R}_0 = \rho(FV^{-1}) = \max\{\mathcal{R}_{0c}, \mathcal{R}_{0m}\}$.

For Covid-19 only models, $\mathcal{R}_{0c}$ is the basic reproduction number, while for TB only models, $\mathcal{R}_{0m}$ is the reproduction number.

4.2 *Stability of the disease-free equilibrium*

4.2.1 Local Stability of DFE

Theorem 4.1 : *The DFE of system (1),* $\mathcal{E}_0$, *is unstable in* Π *if* $\mathcal{R}_0 > 1$ *and locally asymptotically stable if* $\mathcal{R}_0 < 1$.

***Proof*:** The Jacobian matrix the model (1) around DFE point $\mathcal{E}_0$ is given by:

$$J_{\mathcal{E}_0} = \begin{pmatrix} -\mu & -\frac{\beta\Omega}{\mu} & -\frac{\alpha\Omega}{\mu} & -\frac{(\beta+\alpha)\Omega}{\mu} & \delta_1 & \delta_2 & \delta_3 & -\frac{\beta\varepsilon\Omega}{\mu} \\ 0 & \frac{\beta\Omega}{\mu}-\varsigma_1 & 0 & \frac{\beta\Omega}{\mu} & 0 & 0 & 0 & \frac{\beta\varepsilon\Omega}{\mu} \\ 0 & 0 & \frac{\alpha\Omega}{\mu}-\varsigma_2 & \frac{\alpha\Omega}{\mu} & 0 & 0 & 0 & 0 \\ 0 & 0 & 0 & -\varsigma_3 & 0 & 0 & 0 & 0 \\ 0 & \sigma_1 & 0 & \varepsilon\varphi & -\delta_1-\mu & 0 & 0 & 0 \\ 0 & 0 & \sigma_2 & 0 & 0 & -\delta_2-\mu & 0 & 0 \\ 0 & 0 & 0 & \varphi(1-\varepsilon)(1-k) & 0 & 0 & -\delta_3-\mu & 0 \\ 0 & \vartheta & 0 & \vartheta & 0 & 0 & 0 & -\tau \end{pmatrix}$$

Here some of the eigenvalues of the matrix $J_{\mathcal{E}_0}$ are $\lambda_1 = -\mu$, $\lambda_2 = -(\delta_3+\mu)$, $\lambda_3 = -(\delta_2+\mu)$, $\lambda_4 = -(\delta_1+\mu)$, $\lambda_5 = -\varsigma_3$, $\lambda_6 = \frac{\alpha\Omega}{\mu} - \varsigma_2$ and the following characteristic polynomials can be used to get the remaining eigenvalues.

$$\lambda^2 + \Upsilon_1\lambda + \Upsilon_2 = 0 \tag{3}$$

where

$$\Upsilon_1 = \frac{\Omega\beta - \mu\tau(\vartheta+\eta_1+\sigma_1)}{\mu} = (\mu+\vartheta+\eta_1+\sigma_1)\left[\left(\frac{\mu\tau}{\varepsilon\vartheta+\tau}\right)\mathcal{R}_{0c} - 1 - \frac{\tau}{\mu+\vartheta+\eta_1+\sigma_1}\right],$$

$$\Upsilon_2 = \frac{\Omega\beta(\varepsilon\vartheta+\tau) - \mu\tau(\mu+\vartheta+\eta_1+\sigma_1)}{\mu} = \tau(\mu+\vartheta+\eta_1+\sigma_1)(\mathcal{R}_{0c}-1).$$

Therefore, whenever $\mathcal{R}_{0m} < 1$(i.e $\lambda_6 < 0$ mean $\frac{\alpha\Omega}{\mu} - (\eta_2+\sigma_2+\mu) = (\eta_2+\sigma_2+\mu)(\mathcal{R}_{0m}-1)$ and $\mathcal{R}_{0c} < 1$ applying the Routh-Hurwitz criterion $\Upsilon_1 > 0$ and $\Upsilon_2 > 0$ the DFE becomes locally asymptotically stable. This result agrees with result of the research by [36]. □

4.2.2 Global Stability of DFE

We explore the global asymptotic stability of the DFE of the model using Castillo-Chavez et. al. [39] approach. Let's recast the model in equation (1) as

$$\frac{d\mathcal{X}}{dt} = \mathcal{F}(\mathcal{X}, \mathcal{Z}),$$
$$\frac{d\mathcal{Z}}{dt} = \mathcal{G}(\mathcal{X}, \mathcal{Z}), \quad \mathcal{G}(\mathcal{X}, 0) = 0.$$

where $\mathcal{X} = (\mathcal{S}, \mathcal{R}_c, \mathcal{R}_m, \mathcal{R}_{cm})$ denotes the number of uninfected components and $\mathcal{Z} = (\mathcal{I}_c, \mathcal{I}_m, \mathcal{I}_{cm}, \mathcal{P})$ denotes the number of infected components. Let $\mathcal{E}_0 = (\mathcal{X}^*, 0)$ represents the DFE point of the system. Whenever the conditions $(\mathcal{H}_1)$ and $(\mathcal{H}_2)$ below are met, the DFE point $\mathcal{E}_0$ is a globally asymptotically stable equilibrium for the model [39]:

$\mathcal{H}_1$: For $\frac{d\mathcal{X}}{dt} = \mathcal{F}(\mathcal{X}, 0), \mathcal{X}^*$ is globally asymptotically stable.

$\mathcal{H}_2$: $\frac{d\mathcal{Z}}{dt} = D_{\mathcal{Z}}\mathcal{G}(\mathcal{X}^*, 0)\mathcal{Z} - \hat{\mathcal{G}}(\mathcal{X}, \mathcal{Z}), \hat{\mathcal{G}}(\mathcal{X}, \mathcal{Z}) \geq 0$ for all $(\mathcal{X}, \mathcal{Z}) \in \Pi$.

Now considering $\mathcal{H}_1$, $\frac{d\mathcal{X}}{dt} = \mathcal{F}(\mathcal{X}, 0)$, the reduced system is given by:

$$\mathcal{F}(\mathcal{X}, 0) = \begin{pmatrix} \Omega - \mu\mathcal{S} \\ 0 \\ 0 \\ 0 \end{pmatrix}$$

Therefore, the DFE of system (1), $\mathcal{E}_0 = (\mathcal{X}^*, 0)$ to be globally asymptotically stable. This is because the solution is given by $S(t) = \frac{\Omega}{\mu} + (S(t) - \frac{\Omega}{\mu})e^{-\mu t}$ which converges to $\frac{\Omega}{\mu}$ as $t \to \infty$. From the Next condition $\mathcal{H}_2$, the matrix $D_{\mathcal{Z}}\mathcal{G}(\mathcal{X}^*, 0)$ is calculated us

$$D_{\mathcal{Z}}\mathcal{G}(\mathcal{X}^*, 0) = \begin{pmatrix} \frac{\beta\Omega}{\mu} - \vartheta - \eta_1 - \sigma_1 - \mu & 0 & \frac{\beta\Omega}{\mu} & \frac{\beta\varepsilon\Omega}{\mu} \\ 0 & \frac{\alpha\Omega}{\mu} - \eta_2 - \sigma_2 - \mu & \frac{\alpha\Omega}{\mu} & 0 \\ 0 & 0 & -\mu - \varphi - \vartheta - \sigma_1 - \sigma_2 & 0 \\ \vartheta & 0 & \vartheta & -\tau \end{pmatrix}$$

Then column vector $\hat{\mathcal{G}}(\mathcal{X}, \mathcal{Z})$ is given by

$$\hat{\mathcal{G}}(\mathcal{X}, \mathcal{Z}) = \begin{pmatrix} (\frac{\Omega}{\mu} - \mathcal{S})\alpha\mathcal{I}_m + (\frac{\Omega}{\mu} - S)\alpha\mathcal{I}_{cm} + \beta(\mathcal{I}_c + \mathcal{I}_{cm} + \varepsilon V)\mathcal{I}_m \\ (\frac{\Omega}{\mu} - S)\beta\mathcal{I}_c + (\frac{\Omega}{\mu} - \mathcal{S})\beta\mathcal{I}_{cm} + (\frac{\Omega}{\mu} - \mathcal{S})\beta\varepsilon\mathcal{P} + \alpha(\mathcal{I}_m + \mathcal{I}_{cm})\mathcal{I}_c \\ -((\mu + \varphi + \vartheta + \sigma_1 + \sigma_2)\mathcal{I}_{cm} + \alpha(\mathcal{I}_m + \mathcal{I}_{cm})\mathcal{I}_c + \beta(I_c + \mathcal{I}_{cm} + \varepsilon\mathcal{V})\mathcal{I}_m)) \\ 0 \end{pmatrix}$$

(4)

From equation (4) the third entries of $\hat{\mathcal{G}}(\mathcal{X},\mathcal{Z})$ are negative if all the parameters and the state variables in those entries are taken strictly positive. As a result, the second criterion $(\mathcal{H}_2)$ stated above is not met and it can be deduced that the DFE might not be globally asymptotically stable. Thus, the following conclusion will be drawn.

Theorem 4.2 : *The DFE point* $\mathcal{E}_0 = (\mathcal{X}^*, 0)$ *of system (1),* $\mathcal{E}_0$, *is not globally asymptotically stable.*

4.3 *Possible existence of backward bifurcation*

It is possible to demonstrate the occurrence of backward bifurcation on systems (1) with the use of the center manifold theory [39–42]. We specifically used Castillo-Chavez and Song's theory [39]. First, making a transformation of variables of the system (1), we have $x_1 = \mathcal{S}$, $x_2 = \mathcal{I}_c$, $x_3 = \mathcal{I}_m$, $x_4 = \mathcal{I}_{cm}$, $x_5 = \mathcal{R}_c$, $x_6 = \mathcal{R}_m$, $x_7 = \mathcal{R}_{cm}$, $x_8 = \mathcal{P}$ with vector representation of $\mathbf{x} = (x_1, x_2, x_3, x_4, x_5, x_6, x_7, x_8)^T$. If the model is denoted by $\frac{d\mathbf{x}}{dt} = \mathbf{f}(\mathbf{x})$ with $\mathbf{f}(\mathbf{x}) = (f_1(\mathbf{x}),\ f_2(\mathbf{x}),\ f_3(\mathbf{x}),\ f_4(\mathbf{x}),\ f_5(\mathbf{x}),\ f_6(\mathbf{x}),\ f_7(\mathbf{x}),\ f_8(\mathbf{x}))^T$. Hence

$$\begin{cases} \frac{dx_1}{dt} &= f_1 = \ \Omega + \delta_2 x_6 + \delta_1 x_5 + \delta_3 x_7 - (\lambda_1 + \lambda_2)x_1 - \mu x_1 \\ \frac{dx_2}{dt} &= f_2 = \ \lambda_1 x_2 - \lambda_2 x_2 - (\vartheta + \eta_1 + \sigma_1 + \mu)x_2 \\ \frac{dx_3}{dt} &= f_3 = \ \lambda_1 x_1 - \lambda_2 x_3 - (\eta_2 + \sigma_2 + \mu)x_3 \\ \frac{dx_4}{dt} &= f_4 = \ \lambda_1 x_2 + \lambda_2 x_3 - (\vartheta + \varphi + \sigma + \mu)x_4 \\ \frac{dx_5}{dt} &= f_5 = \ \sigma_1 x_2 + \varepsilon\varphi x_4 - (\delta_1 + \mu)x_5 \\ \frac{dx_6}{dt} &= f_6 = \ \sigma_2 x_3 + (1-\varepsilon)\varphi k x_4 - (\delta_2 + \mu)x_6 \\ \frac{dx_7}{dt} &= f_7 = \ \varphi(1-\varepsilon)(1-k)x_4 - (\delta_3 + \mu)x_7 \\ \frac{dx_8}{dt} &= f_8 = \ \vartheta(x_2 + x_4) - \tau \cdot x_8 \end{cases} \tag{5}$$

Let

$$\beta^* = \frac{\mu\tau(\vartheta+\eta_1+\sigma_1+\mu)}{\Omega(\varepsilon\vartheta+\tau)} \qquad \alpha^* = \frac{\mu(\eta_2+\sigma_2+\mu)}{\Omega}$$

be the bifurcation parameters solved at $\mathcal{R}_{0c} = 1$ and $\mathcal{R}_{0m} = 1$ (i.e $\mathcal{R}_0 = 1$). Then the Jacobian of system (5) at DFE is given by:

$$J_{\mathcal{E}_0} = \begin{pmatrix} -\mu & -\frac{\beta^*\Omega}{\mu} & -\frac{\alpha^*\Omega}{\mu} & -\frac{(\beta^*+\alpha^*)\Omega}{\mu} & \delta_1 & \delta_2 & \delta_3 & -\frac{\beta^*\varepsilon\Omega}{\mu} \\ 0 & \frac{\beta^*\Omega}{\mu}-\varsigma_1 & 0 & \frac{\beta^*\Omega}{\mu} & 0 & 0 & 0 & \frac{\beta^*\varepsilon\Omega}{\mu} \\ 0 & 0 & \frac{\alpha^*\Omega}{\mu}-\varsigma_2 & \frac{\alpha^*\Omega}{\mu} & 0 & 0 & 0 & 0 \\ 0 & 0 & 0 & -\varsigma_3 & 0 & 0 & 0 & 0 \\ 0 & \sigma_1 & 0 & \varepsilon\varphi & -\delta_1-\mu & 0 & 0 & 0 \\ 0 & 0 & \sigma_2 & 0 & 0 & -\delta_2-\mu & 0 & 0 \\ 0 & 0 & 0 & \varphi(1-\varepsilon)(1-k) & 0 & 0 & -\delta_3-\mu & 0 \\ 0 & \vartheta & 0 & \vartheta & 0 & 0 & 0 & -\tau \end{pmatrix}$$

Computing the right eigenvector $\mathbf{w} = (w_1, w_2, w_3, w_4, w_5, w_6, w_7, w_8)^T$ it is obtained that

$$\begin{gathered} w_1 = -\frac{\beta\varepsilon\vartheta\Omega+\beta\tau\Omega}{\mu\tau}w_2, w_2 = w_2, w_8 = \frac{\vartheta}{\tau}w_2 \\ w_3 = w_4 = w_5 = w_6 = w_7 = 0,. \end{gathered} \tag{6}$$

And the left eigenvector $\mathbf{v} = (v_1, v_2, v_3, v_4, v_5, v_6, v_7, v_8)^T$ is given as

$$\begin{gathered} v_1 = v_3 = v_5 = v_6 = v_7 = 0, \\ v_2 = v_2, v_4 = \frac{\beta\vartheta\varepsilon\Omega+\beta\tau\Omega}{\mu\tau(\vartheta+\varphi+\sigma_1+\sigma_2+\mu)}v_2, v_8 = \frac{\beta\varepsilon\Omega}{\mu\tau}v_2. \end{gathered} \tag{7}$$

Using Theorem 4.1 in [39], in system (5) the only crucial ones and non-zero derivative evaluated at $(\mathcal{E}_0, \beta^*, \alpha^*)$ are given below.

$$\begin{gathered} \frac{\partial^2 f_2}{\partial x_1 \partial x_2} = \frac{\partial^2 f_2}{\partial x_2 \partial x_1} = \beta^*, \ \frac{\partial^2 f_2}{\partial x_2 \partial x_3} = \frac{\partial^2 f_2}{\partial x_3 \partial x_2} = -\alpha, \frac{\partial^2 f_2}{\partial x_1 \partial x_8} = \frac{\partial^2 f_2}{\partial x_8 \partial x_1} = \beta\varepsilon, \\ \frac{\partial^2 f_4}{\partial x_2 \partial x_3} = \frac{\partial^2 f_4}{\partial x_3 \partial x_2} = \beta^* + \alpha^*, \ \frac{\partial^2 f_4}{\partial x_2 \partial x_4} = \frac{\partial^2 f_4}{\partial x_4 \partial x_2} = \alpha^*, \\ \frac{\partial^2 f_4}{\partial x_3 \partial x_4} = \frac{\partial^2 f_4}{\partial x_4 \partial x_3} = \beta^*, \ \frac{\partial^2 f_4}{\partial x_8 \partial x_3} = \frac{\partial^2 f_4}{\partial x_3 \partial x_8} = \beta^*\varepsilon \end{gathered} \tag{8}$$

Additionally,

$$\frac{\partial^2 f_2}{\partial x_2 \partial \beta} = \frac{\partial^2 f_2}{\partial \beta \partial x_2} = \frac{\Omega}{\mu}, \ \frac{\partial^2 f_2}{\partial x_3 \partial \alpha} = \frac{\partial^2 f_2}{\partial \alpha \partial x_3} = -\alpha, \frac{\partial^2 f_2}{\partial x_8 \partial \beta} = \frac{\partial^2 f_2}{\partial \beta \partial x_8} = \frac{\Omega}{\mu}, \tag{9}$$

Thus, using equations (6), (7), (8) and (9) coefficient a is obtained

$$a = \sum_{k,i,j=1}^{10} v_k w_i w_j \frac{\partial f_k}{\partial x_i \partial x_j} = 2v_2 w_2 w_1 \beta^* - 2v_2 w_1 w_8 \beta^* \varepsilon = 2\left(\frac{(\varepsilon\vartheta\Omega + \tau\Omega)\vartheta\varepsilon}{\mu^2\tau^2} - \frac{\varepsilon\vartheta\Omega + \tau\Omega}{\mu^2\tau} w_2 \right) \tag{10}$$

and

$$b = \sum_{k,i=1}^{10} v_k w_i \frac{\partial f_k}{\partial x_i \partial \beta} = v_2 w_2 \frac{\Omega}{\mu} + v_2 w_8 \frac{\Omega}{\mu} = \frac{\Omega}{\mu} + \frac{\vartheta}{\tau}\frac{\Omega}{\mu} \tag{11}$$

It is clear from equation (11) that the bifurcation coefficient, *b*, is automatically positive. Thus, it follows from Theorem 4.1 in [39] that the TB-COVID 19 co-infection model will undergo backward bifurcation if the bifurcation coefficient, *a*, given by equation (10), is positive.

Theorem 4.3 : *The coinfection model (1)undergoes a subcritical (backward) bifurcation as* $\mathcal{R}_0$ *crosses unity, whenever the coefficient* $a > 0$ *and* $b > 0$. *Hence, the following result will be established.*

4.4 *Sensitivity Analysis*

In this subsection, we analyse the effect of different model parameters to specify the comparative impact of these parameters in the disease transmission. The sensitivity indices of $\mathcal{R}_0$ with respect to the parameters are calculated, using the normalized forward sensitivity index formula $\Lambda_y^{\mathcal{R}_0}$, where *y* is the model parameter, following the technique described in [43, 44]. These indices is a crucial tool to determine the model robustness to parameter values. Since $\mathcal{R}_0 = max\{\mathcal{R}_{0c}, \mathcal{R}_{0m}\}$, we obtained the sensitivity indices of $\mathcal{R}_{0c}$ and $\mathcal{R}_{0m}$ separately:

$$\mathcal{R}_{0c} = \frac{\Omega\beta(\varepsilon\vartheta + \tau)}{\mu\tau(\vartheta + \eta_1 + \sigma_1 + \mu)} \qquad \mathcal{R}_{0m} = \frac{\alpha\Omega}{\mu(\eta_2 + \sigma_2 + \mu)}$$

$$\begin{cases} \Lambda_{\beta}^{\mathcal{R}_{0c}} = \dfrac{\mathcal{R}_{0c}}{\partial\beta}\times\dfrac{\beta}{\mathcal{R}_{0c}} = 1 > 0 \\ \Lambda_{\varepsilon}^{\mathcal{R}_{0c}} = \dfrac{\mathcal{R}_{0c}}{\partial\varepsilon}\times\dfrac{\varepsilon}{\mathcal{R}_{0h}} = \dfrac{\varepsilon\vartheta}{\varepsilon\vartheta+\tau} > 0 \\ \Lambda_{\vartheta}^{\mathcal{R}_{0c}} = \dfrac{\mathcal{R}_{0c}}{\partial\vartheta}\times\dfrac{\vartheta}{\mathcal{R}_{0c}} = \dfrac{(\tau-\varepsilon\mu+\varepsilon\eta_1+\varepsilon\sigma_1)\vartheta}{(\vartheta+\eta_1+\sigma_1+\mu)(\varepsilon\vartheta+\tau)} > 0 \\ \Lambda_{\tau}^{\Re_{0c}} = \dfrac{\partial\Re_{0c}}{\partial\tau}\times\dfrac{\tau}{\Re_{0c}} = -\dfrac{\varepsilon\vartheta}{\varepsilon\vartheta+\tau} < 0 \\ \Lambda_{\sigma_1}^{\mathcal{R}_{0c}} = \dfrac{\partial\mathcal{R}_{0c}}{\partial\sigma}\times\dfrac{\sigma_1}{\mathcal{R}_{0c}} = -\dfrac{\sigma_1}{\vartheta+\eta_1+\sigma_1+\mu} < 0 \\ \Lambda_{\mu}^{\mathcal{R}_{0c}} = \dfrac{\partial\mathcal{R}_{0c}}{\partial\mu}\times\dfrac{\mu}{\Re_{0c}} = -\dfrac{\vartheta+\eta_1+\sigma_1+2\mu}{\vartheta+\eta_1+\sigma_1+\mu} < 0 \end{cases} \quad \begin{cases} \Lambda_{\alpha}^{\mathcal{R}_{0m}} = \dfrac{\partial\mathcal{R}_{0m}}{\partial\alpha}\times\dfrac{\alpha}{\mathcal{R}_{0m}} = 1 > 0 \\ \Lambda_{\mu}^{\mathcal{R}_{0m}} = \dfrac{\partial\mathcal{R}_{0m}}{\partial\mu}\times\dfrac{\mu}{\mathcal{R}_{0m}} = -\dfrac{\eta_2+\sigma_2+2\mu}{\eta_2+\sigma_2+\mu} < 0 \\ \Lambda_{\sigma_2}^{\mathcal{R}_{0m}} = \dfrac{\partial\mathcal{R}_{0m}}{\partial\sigma_2}\times\dfrac{\sigma_2}{\mathcal{R}_{0m}} = -\dfrac{\sigma_2}{\eta_2+\sigma_2+\mu} < 0 \\ \Lambda_{\eta_2}^{\mathcal{R}_{0m}} = \dfrac{\partial\mathcal{R}_{0m}}{\partial\eta_2}\times\dfrac{\eta_2}{\mathcal{R}_{0m}} = -\dfrac{\eta_2}{\eta_2+\sigma_2+\mu} < 0 \end{cases}$$

Examining the sensitivity analysis, it is biologically reasonable to suggest that decreasing β, α, ε and ϑ in order to control the disease. The other possible sensitive parameters that are important for effective control of the disease are increasing $\vartheta, \tau_2, \sigma_2, \varphi$.

From Figure 1, the reproduction rates increase as the parameter value goes up when the sensitivity index is positive. In other words, if positive index parameters' values rise, they have the potential to spread the coinfection disease. Conversely, if the sensitivity index is negative, reproduction will decrease as the parameter value increases. This implies that as the value of negative index parameters rises, so does their potential to reduce the burden of coinfection disease on the community. Based on this information, decision-makers and other stakeholders are expected to take appropriate action to address Covid-19 infection, TB infection and their co-infection in the community.

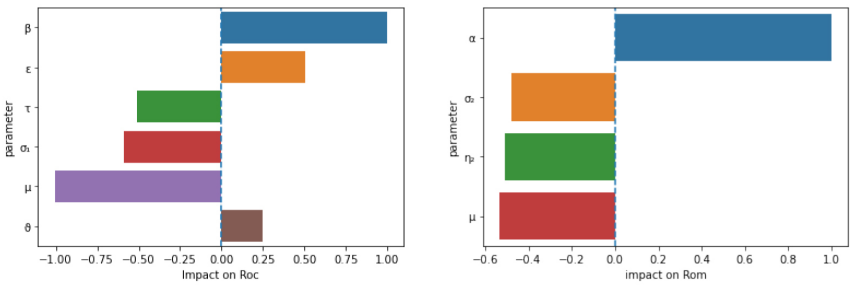

Figure 1

Magnitude and direction of sensitivity analysis results of parameters for (a) Covid-19 and (b) TB explicit models.

5. Numerical Simulations

We have explored the analytical behaviors of the proposed mathematical model in equation (1) in the above sections. Here, we employ the ode45 package of Maple to carry out numerical simulation of the mentioned co-infection model. We do this by using all parameter values mentioned in Table 1 as well as the initial values of the state variables for the model equations $\mathcal{S}(0) = 1000,\ \mathcal{I}_c(0) = 10,\ \mathcal{R}_c(0) = 10,\ \mathcal{I}_{cm}(0) = 10,$ $\mathcal{I}_m(0) = 100,\ \mathcal{R}_m(0) = 10,\ \mathcal{R}_{cm}(0) = 5,\ \mathcal{V}(0) = 1000.$

The impact of the rate α on the population of TB-Covid-19 co-infection and TB-only infected individuals is demonstrated in Figure 2. It shows that only TB infected or TB- Covid-19 co-infected increases as the values of the contact rate α rise. We can either follow good hygiene habits or enhance ventilation to lower the contact rate. Government policymakers should view it as a mitigation approach.

Table 1

Parameters values of TB-Covid-19 co-infection model.

Parameter	Description	Value day^{-1}	Source
Ω	Recruitment rate of susceptible humans	150	Assumed
β	Covid-19 transmission rate contact rate	0.25	[35]
α	TB transmission rate	0.065	[28]
φ	Rate of recovery from TB-Covid-19 is co infection diseases	0.002	Assumed
ϑ	Virus shedding rate by Covid-19 infected and coinfected people	0.012	[25]
σ_1	Rate of recovery from Covid-19 is co infection diseases	0.0025	[23, 25]
σ_2	Rate of recovery from TB is co infection diseases	0.545	[19]
$\delta_1, \delta_2, \delta_3$	Loss of imminity for $\mathcal{I}_c, \mathcal{I}_m, \mathcal{I}_{cm}$	varies	Assumed
η_1	Covid-19 induced death rate	0.017	[23]
η_1	TB induced death rate	0.575	[18]
τ	Decay rate of SARSCoV- 2 population	0.85	[25]
μ	Natural death rate of human population	0.016	[21, 22]
ε	Modifying parameter	0.036	[25]

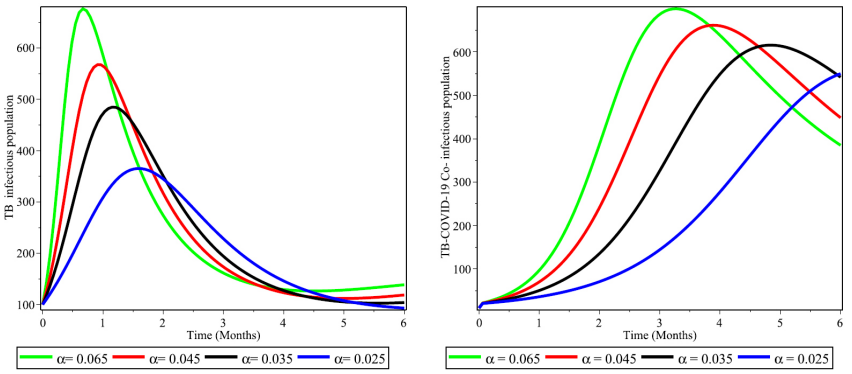

Figure 2

Effect of α on TB infectious and Co-infectious population.

The graph illustrated in Figure 3 the impact of Covid-19 transfer rates β to the population of Covid-19 infection and TB-Covid-19 co-infection. It was shown that an increase in the rate will decrease the number of individuals in that class(Covid-19 infection and TB-Covid-19 co-infection).

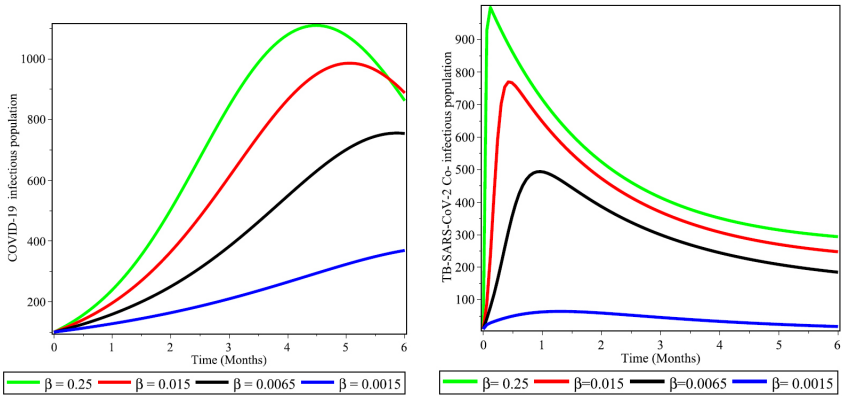

Figure 3

Effect of β on Covid-19 infectious and Co-infectious population.

The impact of the virus shading rate ϑ of $\mathcal{I}_c$, and $\mathcal{I}_{cm}$ on environmental surfaces is shown in Figure 4. It demonstrated that as the rate ϑ increases, the contaminated surfaces or objects in the environment with the number of SARS-CoV-2 virus increases. Therefore, it is important to sanitizer and spray chemicals to clean contaminated surfaces to limit the impact of disease.

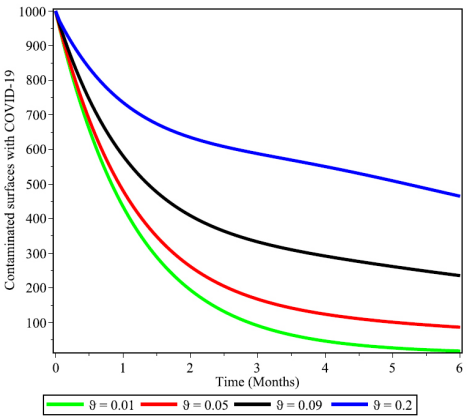

Figure 4

Effect of virus shading rate ϑ on surfaces in the environment.

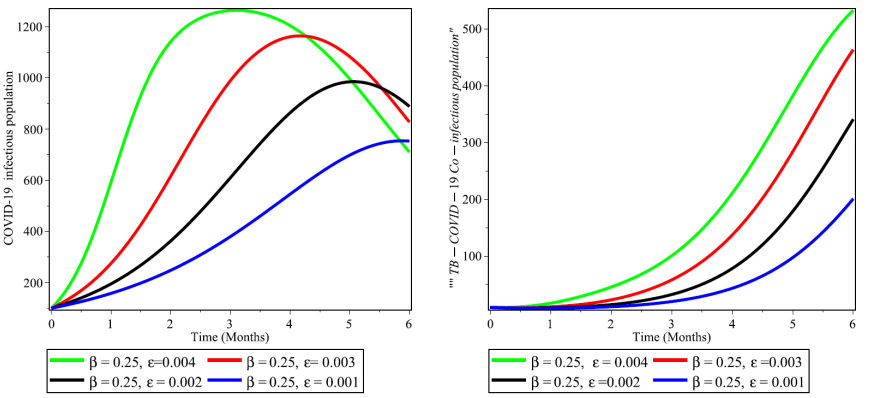

Figure 5

Effect of ε on Covid-19 infectious and co-infectious population.

Figure 5 illustrates how the rate of contaminated surface infection ε affected the spread of Covid-19 only and the TB-Covid-19 co-infection population. It shows decreasing concentration of contaminated surfaces reduces the rate of infection of the Covid-19 only and the co-infected population. Therefore, stakeholders should focus on disinfecting the community's contaminated surfaces, primarily in government sectors where people meet for a service.

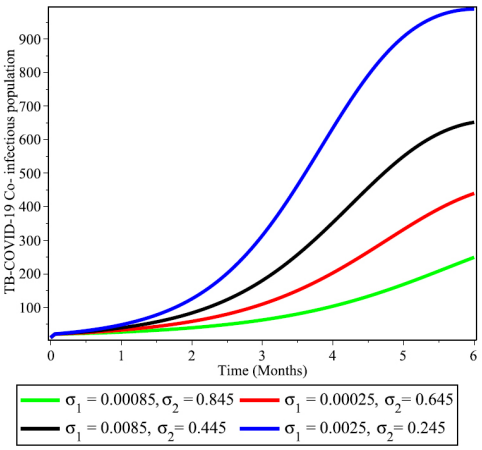

Figure 6

Effect of recovery rate σ_1 and σ_2 on TB- Covid-19 co-infectious population.

Figure 6 demontrates the impact of TB and Covid-19 recovery rates on the co-infected community. Co-infected individuals either recover from TB only, Covid-19 only, or from both diseases with a different probability, as we mentioned in the model description and then they join their respective recovered compartment. As a result, the graph demonstrates that raising the rate of recovery in the co-infected population has a massively important effect on lowering the prevalence of both diseases.

6. Conclusions

We developed a transmission dynamics model for TB-Covid-19 co-infection and the population was subdivided into seven compartments including the effect of contaminated surfaces in the environment. The basic reproduction number is determined using next generation matrix method. Stability analysis of the disease-free equilibrium point was conducted. Also it provided evidence that backward bifurcation exists. We also demonstrated how parameters responded to the basic reproduction number. In terms of numbers, we explored with the impact of key parameters on the growth or control of Covid-19 only, TB only and their co-infection. According to the findings, a significant portion of the reduction in TB-Covid-19 infectious individuals in the community can be attributed to an increase in the rate of TB and Covid-19 recovery (σ_1 and σ_2). We found that reducing the contact rate β has a considerable impact on the infectious population that is co-infected with Covid-19 and TB-

Covid-19. Also, reducing the contact rate α is significant in bringing down the number of TB and TB-Covid-19 co-infected infectious population. Therefore, government stakeholders should place special emphasis on the aforementioned key criteria in order to stop the spread of infection in the community for Covid-19 only, TB only and TB-Covid-19 co-infection.

Acknowledgment

The authors acknowledge the comments of the anonymous reviewers, which increases the quality of the paper.

Competing Interests

The authors declare that there are no conflicts of interest.

Data Availability

The data used in this study are included within the article.

Funding

Not applicable

Authors' contributions

HTA and ZTM participated in the formulation, analysis and drafting of the manuscript. Both the authors have and approved the final manuscript.

References

[1] Ajay Kumar Mishra, Anu Anna George, Kamal Kant Sahu, Amos Lal and George Abraham. Review of clinical profile, risk factors and outcomein patients with tuberculosis and Covid-19. *Acta Bio Medica: Atenei Parmensis*, 92(1), 2021.

[2] World Health Organization et al. Covid-19 weekly epidemiological update, 25 May 2021. 2021.

[3] Centers for Disease Control and Prevention (CDC). Infection prevention and control in the household management of people with suspected or confirmed coronavirus disease (Covid-19). Atlanta:

CDC;2020[cited 2020 22 Aprile], Available from: https://www.cdc.gov/coronavirus/2019-ncov/downloads/2019-ncov-factsheet.pdf.

[4] Hyun Mo Yang, Luis Pedro Lombardi Junior, Fabio Fernandes Morato Castro and Ariana Campos Yang. Mathematical modeling of the transmission of sars-cov-2—evaluating the impact of isolation in são paulo state (Brazil) and lockdown in spain associated with protective measures on the epidemic of Covid-19. *Plos one*, 16(6):e0252271, 2021.

[5] World Health Organization et al. Global tuberculosis report 2020. 2020.

[6] World Health Organization et al. Anti-tuberculosis drug resistance in the world: third global report. Technical report, World Health Organization, 2004.

[7] James A Seddon, Lillian Tugume, Regan Solomons, Kameshwar Prasad, Nathan C Bahr, Tuberculous Meningitis International Research Consortium, et al. The current global situation for tuberculous meningitis: epidemiology, diagnostics, treatment and outcomes. *Wellcome Open Research*, 4, 2019.

[8] Joseph Donovan, Guy E Thwaites and Julie Huynh. Tuberculous meningitis: where to from here? *Current Opinion in Infectious Diseases*, 33(3):259, 2020.

[9] Farida Essajee, Regan Solomons, Pierre Goussard and Ronald Van Toorn. Child with tuberculous meningitis and Covid-19 coinfection complicated by extensive cerebral sinus venous thrombosis. *BMJ Case Reports CP*, 13(9):e238597, 2020.

[10] Radu Crisan-Dabija, Cristina Grigorescu, Cristina-Alice Pavel, Bogdan Artene, Iolanda Valentina Popa andrei Cernomaz and Alexandru Burlacu. Tuberculosis and Covid-19: lessons from the past viral outbreaks and possible future outcomes. *Canadian Respiratory Journal*, 2020, 2020.

[11] José Arturo Martínez Orozco, Ángel Sánchez Tinajero, Eduardo Becerril Vargas andrea Iraís Delgado Cueva, Héctor Reséndiz Escobar, Eduardo Vázquez Alcocer, Luis Armando Narváez Díaz and Danna Patricia Ruiz Santillán. Covid-19 and tuberculosis coinfection in a 51-year-old taxi driver in mexico city. *The American Journal of Case Reports*, 21:e927628–1, 2020.

[12] Wan-mei Song, Jing-Yu Zhao, Qian-Yun Zhang, Si-Qi Liu, Xue-Han Zhu, Qi-Qi An, Ting-Ting Xu, Shi-jin Li, Jin-yue Liu, Ning-ning Tao, et al. Covid-19 and tuberculosis coinfection: An overview of case reports/case series and meta-analysis. *Frontiers in Medicine*, 8, 2021.

[13] Monika Kozińska and Ewa Augustynowicz-Kopeć. Covid-19 in patients with active tuberculosis. *Diagnostics*, 11(10):1768, 2021.

[14] Alkesh Kumar Khurana and Deepak Aggarwal. The (in) significance of tb and Covid-19 co-infection. *European Respiratory Journal*, 56(2), 2020.

[15] Ayoub Maaroufi, Abdellatif Diai, Nouredine Jebbar, Lotfi Bibiche, Kaissi Jaber, Nabil Jbili, Hicham Kechna and Jaouad Laoutid. Tuberculous meningitis and Covid-19 co-infection: About a case. *Open Journal of Clinical Diagnostics*, 11(2):52–58, 2021.

[16] Felix Okoe Mettle, Prince Osei Affi and Clement Twumasi. Modelling the transmission dynamics of tuberculosis in the ashanti region of ghana. *Interdisciplinary Perspectives on Infectious Diseases*, 2020, 2020.

[17] Doyo Kereyu and Seleshi Demie. Transmission dynamics model of tuberculosis with optimal control strategies in haramaya district, ethiopia. *Advances in Difference Equations*, 2021(1):1–22, 2021.

[18] Muhammad Altaf Khan Fatmawati, Ebenezer Bonyah, Zakia Hammouch and Endrik Mifta Shaiful. A mathematical model of tuberculosis (tb) transmission with children and adults groups: a fractional model. *Aims Math,* 5(4):2813–2842, 2020.

[19] Ashenafi Kelemu Mengistu and Peter J Witbooi. Modeling the effects of vaccination and treatment on tuberculosis transmission dynamics. *Journal of Applied Mathematics,* 2019, 2019.

[20] BiBi Fatima, Manar A Alqudah, Gul Zaman, Fahd Jarad and Thabet Abdeljawad. Modeling the transmission dynamics of middle eastern respiratory syndrome coronavirus with the impact of media coverage. *Results in Physics*, 24:104053, 2021.

[21] Getachew Teshome Tilahun and Haileyesus Tessema Alemneh. Mathematical modeling and optimal control analysis of Covid-19 in ethiopia. *Journal of Interdisciplinary Mathematics,* pages 1–20, 2021.

[22] Issaka Haruna, Haileyesus Tessema Alemneh and Getachew Teshome Tilahun. The effect of quarantine and treatment in Covid-19 transmission: from mathematical modeling perspective. *Commun. Math. Biol. Neurosci.*, 2021:Article–ID, 2021.

[23] Aychew Wondyfraw Tesfaye and Tesfaye Sama Satana. Stochastic model of the transmission dynamics of Covid-19 pandemic. *Advances in Difference Equations,* 2021(1):1–21, 2021.

[24] Samuel Mwalili, Mark Kimathi, Viona Ojiambo, Duncan Gathungu and Rachel Mbogo. Seir model for Covid-19 dynamics incorporating

the environment and social distancing. *BMC Research Notes*, 13(1):1–5, 2020.

[25] Kassahun Getnet Mekonen, Tatek Getachew Habtemicheal and Shiferaw Feyissa Balcha. Modeling the effect of contaminated objects for the transmission dynamics of Covid-19 pandemic with self protection behaviour changes. *Results in Applied Mathematics*, 9:100134, 2021.

[26] Rubayyi T Alqahtani. Mathematical model of sir epidemic system (Covid-19) with fractional derivative: stability and numerical analysis. *Advances in Difference Equations*, 2021(1):1–16, 2021.

[27] Juliane F Oliveira, Daniel CP Jorge, Rafael V Veiga, Moreno S Rodrigues, Matheus F Torquato, Nivea B da Silva, Rosemeire L Fiaccone, Luciana L Cardim, Felipe AC Pereira, Caio P de Castro, et al. Mathematical modeling of Covid-19 in 14.8 million individuals in bahia, brazil. *Nature Communications*, 12(1):1–13, 2021.

[28] J Nainggolan, Sudradjat Supian, AK Supriatna and N Anggriani. Mathematical model of tuberculosis transmission with reccurent infection and vaccination. In *Journal of Physics: Conference Series*, volume 423, page 012059. IOP Publishing, 2013.

[29] S Bowong and J Kurths. Modelling tuberculosis and hepatitis b co-infections. *Mathematical Modelling of Natural Phenomena*, 5(6):196–242, 2010.

[30] Nita H Shah, Nisha Sheoran and Yash Shah. Dynamics of hiv-tb co-infection model. *Axioms*, 9(1):29, 2020.

[31] Ibrahim M Hezam, Abdelaziz Foul and Adel Alrasheedi. A dynamic optimal control model for Covid-19 and cholera co-infection in yemen. *Advances in Difference Equations*, 2021(1):1–30, 2021.

[32] A Omame, H Rwezaura, ML Diagne, SC Inyama and JM Tchuenche. Covid-19 and dengue co-infection in brazil: optimal control and cost-effectiveness analysis. *The European Physical Journal Plus*, 136(10):1–33, 2021.

[33] SY Tchoumi, ML Diagne, H Rwezaura and JM Tchuenche. Malaria and Covid-19 co-dynamics: A mathematical model and optimal control. *Applied Mathematical Modelling*, 99:294–327, 2021.

[34] Bhavnita Soni and Shailza Singh. Covid-19 co-infection mathematical model as guided through signalling structural framework. *Computational and Structural Biotechnology Journal*, 19:1672–1683, 2021.

[35] Andrew Omame, Ndolane Sene, Ikenna Nometa, Cosmas I Nwakanma, Emmanuel U Nwafor, Nneka O Iheonu and Daniel Okuonghae. Analysis of Covid-19 and comorbidity co-infection model with optimal control. *Optimal Control Applications and Methods*, 2020.

[36] A Omame, M Abbas and CP Onyenegecha. A fractional-order model for Covid-19 and tuberculosis co-infection using atangana-baleanu derivative. *Chaos, Solitons & Fractals*, page 111486, 2021.

[37] Pauline Van den Driessche and James Watmough. Reproduction numbers and sub-threshold endemic equilibria for compartmental models of disease transmission. *Mathematical Biosciences*, 180(1-2):29–48, 2002.

[38] Haileyesus Tessema Alemneh. A co-infection model of dengue and leptospirosis diseases. *Advances in Difference Equations*, 2020(1):1–23, 2020.

[39] Carlos Castillo-Chavez and Baojun Song. Dynamical models of tuberculosis and their applications. *Mathematical Biosciences and Engineering*, 1(2):361–404, 2004.

[40] J Carr. Applications of centre manifold theory. SPRINGER'S, 1981.

[41] Jonathan Dushoff, Wenzhang Huang and Carlos Castillo-Chavez. Backwards bifurcations and catastrophe in simple models of fatal diseases. *Journal of Mathematical Biology*, 36(3):227–248, 1998.

[42] Zinabu Teka Melese and Haileyesus Tessema Alemneh. Enhancing reservoir control in the co-dynamics of hiv-vl: from mathematical modeling perspective. *Advances in Difference Equations*, 2021(1):1–20, 2021.

[43] S. M. Blower and H. Dowlatabadi. Sensitivity and uncertainty analysis of complex models of disease transmission: an hiv model, as an example. *International Statistical Review/Revue Internationale de Statistique*, pages 229–243, 1994.

[44] Haileyesus Tessema Alemneh and Negesse Yizengaw Alemu. Mathematical modeling with optimal control analysis of social media addiction. *Infectious Disease Modelling*, 6:405–419, 2021.

Received February, 2022
Revised July, 2022